# New Side Chain Design for pH-Responsive Block Copolymers for Drug Delivery

Priyanka Ray, Narendra Kale, Mohiuddin Quadir \*

Department of Coatings and Polymeric Materials, North Dakota State University, Fargo ND

58108

KEYWORDS: amphiphilic block copolymers, pH-responsive, self-assembly, nanoparticles.

Statistical summary: Total number of words: 5,769; Tables: 2; Scheme and Figures: 6

Correspondence: Phone: (701) 231-6283; E-mail: mohiuddin.quadir@ndsu.edu

**ABSTRACT:** New molecular motifs that can act as pH-regulating triggers for amphiphilic, pHsensitive block copolymers are investigated. Inspired by the mechanism of action of pHindicators, such as methyl orange, and natural amino acids, we designed these copolymers where either 4-Amino-4'-dimethylaminoazobenzene, AZB (pKa 3.4, an amine derivative of methyl orange), isoleucine, Ile (p $K_a$  2.37 for carboxylic acid), or a statistical mixture of the both were appended as side chains to the hydrophobic block to act as pH-triggers. These new side chain motifs were identified with an aim to enhance the self-assembling properties of these block copolymers in terms of particle size and stability, and drug encapsulation and release. As the parent polymer, poly (ethylene) glycol-block- poly (carbonate) (PEG-b-PC) of number average molecular weight 12.1 kDa was used. We observed that when PEG-b-PC block copolymers, when engineered with AZB or Ile-type of pH-regulators appended as side chains at PC blocks, were able to form self-assembled, spherical nanoparticles with hydrodynamic diameters ranging from 114 -137 nm depending on copolymer composition. Critical aggregation concentration (CAC) of block copolymers were found to be governed by the type and content of side chains. We explored the use of these newly designed block copolymer assemblies as drug carriers using gemcitabine (GEM) as a model cytotoxic drug used for pancreatic ductal adenocarcinoma (PDAC). We showed that AZB and Ile decorated copolymeric nanocarriers were able to encapsulate GEM at 13.8 to 28.8 % loading content and release the drug in a pH-dependent pattern. Drug-loaded nanocarriers showed cellular entry into PDAC cells in vitro and was found to exert cytotoxicity against proliferating cancer cells. Drug-free nanocarriers, as well as block copolymers bearing these new pH-responsive triggers did not show any cytotoxicity at usable concentration, thereby reflecting the potentials of these molecular motifs for designing stimuli-responsive drug delivery nanosystems.

# INTRODUCTION

Polymeric nanocarriers have emerged as promising candidates for drug delivery over last several decades 1-4 With the advent of newer polymerization techniques and catalysts, chemically diverse macromolecular constructs have been synthesized with significant bio-functional attributes<sup>5</sup>, such as, diseasetargeting<sup>6, 7</sup>, tissue penetration and localization<sup>6, 8</sup>, drug encapsulation and programmed release at pathological targets. To promote selective delivery and accumulation of drugs to a specific set of diseased tissue, polymeric carriers have been engineered with passive (size-dependent), active (ligand-based), as well as with microenvironment-sensitive targeting modalities.<sup>9-11</sup> For cancer, mono- or multiple-stimuli sensitive drug carriers have found special interest owing to disease heterogeneity, which oftentimes show variable phenotypic disposition of diverse biochemical abnormalities. At nanoscale, stimuli-driven polymeric drug carriers sense these altered biochemical cues, and translate the signal through structural changes that initiate drug release at target site <sup>12, 13</sup>. Both exogenous (such as, temperature gradient, changes in magnetic field, ultrasound intensity, light or electric pulses)<sup>14</sup> or endogenous (pH<sup>6, 15-18</sup>, hypoxia<sup>19-21</sup> or enzyme concentration<sup>22, 23</sup>) stimuli can be used as triggers, and the sensing modalities are generally included either within the primary chain or in the side chains of these polymers to induce drug release on-site, on-demand. Among these biochemical stimuli, the pH-status of target tissues has been heavily investigated as an induction signal for drug release. The design principle of pH-sensitive nanocarriers are based on the fact that a steep pH gradient exists between target and non-target tissues 17, <sup>24-29</sup> <sup>30, 31</sup>. Such gradient is indeed observed and reported for many diseases including inflammatory conditions and metabolically active cancers. For example, microenvironment of breast, ovarian, and pancreatic cancer are acidified due to the dependence of the malignant cells on aerobic glycolysis and efflux of intracellular acidic byproducts to extracellular spaces <sup>32, 33</sup>. Thus, a large cohort of research endeavor has exploited the pH-abnormality of tumors to design targeted drug therapy that is activated under low pH conditions. 34 35-37 16, 38, 39

The most frequently used molecular attribute that has been employed for constructing pHsensing polymers involves tertiary alkyl amines, immobilized as side chains on block copolymer motifs. Through protonation of amines, these polymeric motifs demonstrate reversible, mesoscale phase transition upon pH-shift from neutral to acidic conditions 40, 41 34, 42-47. These architectures therefore have been employed to design nanocarriers to stabilize small molecular drugs in plasma and release the encapsulated cargo in tumors where pH < 7.4. One of the most common classes of pH-responding small molecules are organic acid/base indicators. Most of these indicators bear substituted amine functional groups that show pH-sensing properties through the formation of charged cationic center, which delocalizes with the aromatic core of the molecule under low pH conditions. However, their use in pH-responsive block copolymer design is relatively underexplored. In our attempt to find out a suitable pH-sensing side chain for poly(ethylene glycol)-block-poly(carbonate) (PEG-b-PC) copolymers, we attempted to explore the feasibility of using 4-Amino-4'-dimethylaminoazobenzene (AZB), a methyl orange derivative with  $pK_a$  value of 3.4. Organic dyes have been utilized as pH-sensitive triggers for several dendritic systems for modulating photo activity. <sup>48-50</sup> We immobilized AZB to the PC blocks of PEG-b-PC copolymers during the post-polymerization reaction. We envisioned that these bulky side chains will not only act as regulators for pH-induced structural destabilization, but will also contribute to controlled drug release. plasma stability and drug loading properties. Natural amino acids are another rich molecular repository from which high to moderately sensitive pH-regulators can be selected for designing pH-sensing copolymeric systems. Basic (i.e. histidine, 1-arginine) or acidic (i.e. 1-aspartic acid, 1-glutamic acid) amino acids has already been reported to act as pH-sensing modality for block copolymer assemblies 51-53. In our case, we were interested to explore the use l-isoleucine (Ile) as additional pH-sensing triggers. When appended to the PC blocks of PEG-b-PC block copolymers through α-amino group, Ile will present an α-carboxylic acid as side chains that can function as proton-sensing functionality. As an essential amino acids widely present in nature, 1-isoleucine is molecular motif most commonly utilized by living systems to induce the formation of  $\alpha$ -helical structures and provide the strongest hydrophobic interaction sites<sup>54</sup>. We hypothesize that, these new side chain motifs, i.e. AZB and Ile, will provide the block copolymer with pH-sensing capability and will also serve as intra- or intermolecular binding sites for non-covalent interactions. Among such interactions, we envision that, AZB and Ile motifs be involved in participating in  $\pi$ - $\pi$  or hydrophobic interactions, respectively, in intra- and intermolecular settings. Such enhanced non-covalent interactions will improve plasma stability, drug loading and pH-sensitive release capacity of polymer-polymer or polymer-drug ensembles. Using gemcitabine (GEM), which is one of the frontline chemotherapies for pancreatic ductal adenocarcinoma (PDAC), we set out to validate our hypothesis. To evaluate the combined effect of AZB and Ile on pH-sensitivity, stability and pH-dependent drug release properties, we co-conjugated both AZB and Ile to the PC blocks of PEG-b-PC copolymers at defined ratio. <sup>55</sup> Finally, we checked cellular compatibility, cytotoxicity and internalization behavior of synthesized block copolymers against pancreatic cancer cell line.

# EXPERIMENTAL

Materials. All chemicals were obtained from Sigma-Aldrich unless otherwise mentioned, and anhydrous solvents were from VWR, EMD Millipore. <sup>1</sup>H NMR spectra were recorded using a Bruker 400 MHz spectrometer with TMS as the internal standard. IR Spectra were recorded using an ATR diamond tip on a Thermo Scientific Nicolet 8700 FTIR instrument. Gel permeation chromatography was done on a GPC system (EcoSEC HLC-8320GPC, Tosoh Bioscience, Japan) using a differential RI detector, employing polystyrene (Agilent EasiVial PS-H 4 ml) as the standard and THF as the eluent with a flow rate of 0.35 mL per minute at 40 °C. The sample concentration used was 1 mg/mL of which 20 μL was injected. DLS measurements were carried out using a Malvern instrument (Malvern ZS 90). UV–Vis and fluorescence spectra were recorded using a Varian UV–vis spectrophotometer and a Fluoro-Log3 fluorescence spectrophotometer, respectively. TEM studies were carried out using a JEOL JEM-2100 LaB6 transmission electron microscope (JEOL USA, Peabody, Massachusetts) with an accelerating voltage of 200 kV.

*Synthesis of block copolymers*. For the synthesis of PEG-b-PC systems appended with AZB or Ile, we followed a previously described protocol<sup>41, 56</sup>. First we synthesized the pentafluorophenol (PFP) protected bis (methoxy propionic acid)<sup>57</sup> monomer (1). Ring opening polymerization of (1) using a macroinitiator, methoxy terminated poly(ethylene glycol) (PEG-OH, Mn=5000 g/mol) (2) generated the PEG-b-PC block copolymer (3) at 52% yield <sup>56</sup>. The hydrophobic PC block of copolymer 3 was postfunctionalized by substituting PFP-ester with either 4-Amino-4'-dimethylaminoazobenzene, AZB (an amine derivative of methyl orange, p $K_a$  3.4) to yield copolymer 4 (PEG-AZB), or with isoleucine, Ile (p $K_a$  2.37) to yield copolymer 5 (PEG-IIe). This is to note that, PFP to AZB or Ile molar ratio was kept at 1: 2 to ensure complete substitution of PFP ester from the block copolymer as indicated by <sup>19</sup>F NMR. To generate a block copolymer system where the hydrophobic block is randomly decorated with AZB and Ile, we reacted 3 with 1:1 stoichiometric mixture of AZB and Ile to synthesize the copolymer 6 (PEG-AZB-IIe). Again, combined molar ratio of AZB and Ile with respect to PFP ester was maintained at 1: 2. <sup>1</sup>H and <sup>19</sup>F NMR spectroscopy was used to characterize the synthesized polymers.

**Determination of pKa of synthesized block copolymers.** For determination of acid-base titration characteristics of block copolymers, we adopted a previously established procedure by Engler et  $al^{40}$ . In this method, pH of a 10 mg/mL solution of polymer 4, 5 or 6 was first reduced to pH 2.0 by adding 0.1 M HCl. At this pH, primary amines of polymer 4 and 6 will be in ionized (protonated), and carboxylic acids of 5 and 6 will be in unionized form. The p $K_a$  values (acid dissociation constant) of block copolymers 4-6 were determined by titrating the aqueous solution of the polymers against 0.1 N sodium hydroxide. The p $K_a$  was calculated by measuring the pH at the half-equivalence (inflection) point of the titration curve.

**Preparation of nanoparticles.** To induce the formation of self-assembled structures from block copolymer **4-6**, non-solvent induced phase separation (nanoprecipitation) method was adopted. In this protocol, the block copolymer was first dissolved in a non-selective solvent which dissolves both blocks (such as DMSO) and then added to a selective solvent (such as PBS, pH 7.4) which dissolves only the

hydrophilic block. Such rapid phase transition induced the formation of nanoparticles<sup>58</sup>. As a representative example, we dissolved 10 mg of PEG-AZB (4), PEG-Ile (5) or PEG-AZB-Ile (6) in 250 µL of DMSO and added this solution drop-wise to 750 µL of PBS buffer (pH 7.4) under constant stirring at room temperature. The resultant solution was transferred to a float-a-lyzer (MWCO 3.5-5 kDa) and allowed to dialyze against ~ 700 mL PBS buffer (pH 7.4) overnight with constant shaking at moderate speed. The solutions were then filtered using a 0.2 µm PES filter and stored for further characterization. **Determination of particle size of block copolymeric nanoparticles.** To determine the hydrodynamic diameter of nanoparticles formed by nanoprecipitation techniques, the particle suspension was analyzed using Dynamic Light Scattering (DLS) at a scattering angle of 90°. For zeta potential measurements a sample concentration of 10 mg/mL was used. The zeta potential of the sample solution was determined in terms of electrophoretic mobility by taking an average of 5 independent readings. Both DLS and zeta potential measurement were carried out in PBS, pH 7.4, at an ionic strength of 0.15 M consisting of 0.01 M phosphate buffer, 0.0027 M potassium chloride, and 0.137 M sodium chloride. For TEM measurements, a drop of the sample was placed on a 300-mesh formvar-carbon coated copper TEM grid (Electron Microscopy Sciences, Hatfield, Pennsylvania, USA) for 1 min and wicked off. Phosphotungstic acid 0.1%, pH adjusted to 7-8, was dropped onto the grid and allowed to stand for 2 minutes and then wicked off.

Stability studies of block copolymeric nanoparticles in the presence of plasma proteins. To ascertain the stability of the nanocarriers in the presence of proteins which are commonly encountered during the systemic lifetime of nanoparticles in circulation, we incubated block copolymeric nanoparticles 10% Fetal Bovine Serum (FBS) solution. Post-incubation particle size was monitored using DLS at regular time intervals for a span of 48 h to evaluate the change of particle size as a function of time.

Determination of Critical Aggregation Constant (CAC) of block copolymers. To evaluate the effect of AZB and Ile sidechains on polymer assembly, we determined the CAC of individual polymers following a previously established protocol <sup>28</sup>. Briefly, 10 μL of a stock solution of 0.1 mM pyrene in dichloro-

methane was measured in individual glass vials and dichloromethane was dried under air. To each of these vials, various measured amounts of polymers were added (stock solution concentration 1 mM) so that the concentrations varied from 0.0019 mM to 0.5 mM and the final concentration of pyrene in each vial was 1 μM. After sonication for 45 min, the vials were kept at room temperature for 3 h before recording the fluorescence spectra. The excitation wavelength was maintained at 337 nm, while the emission intensities at 373 nm and 384 nm were recorded (using a bandwidth of 2.5 nm for both excitation and emission). Fluorescence intensity ratios were plotted against the polymer concentration (in log scale). The break point of the curve was considered as the CAC for each polymer.

Encapsulation of drug and dye within polymeric self-assembly. For the preparation of drug loaded nanoparticles, 10 mg of the respective block copolymer and 5 mg of GEM were dissolved in 250  $\mu$ L of DMSO and the solution was added dropwise to a stirring solution of 750  $\mu$ L PBS buffer at room temperature. The resulting suspension was stirred overnight to ensure maximum drug loading into the assembling nanoparticles. The suspension was then loaded onto micro-centrifuge filters (MWCO 3.5 kDa) and centrifuged at 3000 rpm till complete separation of the filtrate into the lower chamber was observed. The filtrate was analyzed using UV–vis spectroscopy (at  $\lambda_{max} = 275$  nm) to quantify the amount of drug loaded. The slurry in the filter was resuspended using chilled PBS to a concentration of 10 mg/mL and used for drug release and other studies. The loading content was calculated using the following equation:

Loading content(%) 
$$\frac{w}{w} = \frac{\text{Amount of drug loaded}}{\text{Total weight of formulation}} \times 100 \dots (Equation 1)$$

To prepare fluorescent dye loaded nanocarriers of synthesized block copolymers, the same protocol was followed and instead of GEM, 50  $\mu$ L of AlexaFluor-647 (AF-647,  $\lambda_{em}$  = 665 nm) was used. Following overnight stirring in aluminum foil covered vials, the dye-loaded nanoparticle suspension was transferred to Float-A-Lyzer® (MWCO 3.5–5 kDa) and dialyzed against 800 mL PBS under constant agita-

tion at moderate speed. Bulk media was changed at regular intervals till no further discoloration of the media was observed.

In vitro release of encapsulated drug from block copolymeric nanoparticles in the presence of plasma. Release studies of the encapsulated drug was carried out using a formerly established protocol<sup>59</sup>. Briefly, 1 mL of the drug-loaded nanoparticle solution (in PBS) reinforced with 10% v/v FBS were taken in the inner chamber of a Float-A-Lyzer® (MWCO 3.5–5 kDa), while 5 mL of phosphate buffer maintained at desired pH (pH 7.4 or pH 4.5) was used in the outer chamber. From the outer chamber, 1 mL of the solution was withdrawn periodically and replaced by an equal volume of fresh buffer of similar pH to maintain the sink condition. The drug release was measured using UV-Visible absorbance spectroscopy at 275 nm.

In vitro cell culture. The pancreatic cancer cell line, MIA PaCa-2 and a non-cancerous pancreatic cell line, HPNE were purchased from ATCC (American Type Culture Collection) and grown at 37 °C with 5% CO2. Both these cell lines were cultured in DMEM high glucose medium (Thermo Fisher Scientific) supplemented with 10% FBS and 1% antibiotic-antimycotic (Gibco) solution. The cell lines were sub-cultured by enzymatic digestion with 0.25% trypsin/ 1 mM EDTA solution (Thermo Fisher Scientific) when they reached approximately 70% confluency.

Cell viability assay. Cell viability assays were performed for all drug-loaded nanoparticles and the corresponding free drug at an equivalent concentration. Cytotoxicity of bare nanoparticles derived from PEG-AZB (4), PEG-Ile (5) and PEG-AZB-Ile (6) were screened against both MIA PaCa-2 and HPNE cell lines. For these cell lines, 5000 cells/well were seeded in 96-well plates and 24 h later, the cells were treated with different concentrations of drug-free nanoparticles ranging from 1mg/mL to 0.0625 mg/mL. For cell viability assay of drug-loaded nanocarriers, the concentration of free and nanoparticle encapsulated GEM was varied from 0.001 μM to 1 μM. After 72 h post incubation, viability was determined using an MTS assay. Cell viability was calculated using the following equation:

Cell viability (%) = 
$$\frac{\text{Absorbance of test sample}}{\text{Absorbance of control}} \times 100 \dots (Equation 2)$$

Confocal microscopy. Cellular uptake of dye (AF-647)-labelled nanoparticles constituted from block copolymers 4-6 was assessed by confocal fluorescence microscopy. MIA PaCa-2 cells were seeded in ibidi® glass bottom dish (35 mm) at 1 × 10<sup>5</sup> cells per well and grown overnight. Then, cells were incubated with dye-labelled nanoparticles at 37 °C in DMEM high glucose medium for 1, 4, and 24 h. At the end of incubation periods, cells were washed with PBS, fixed with formalin, stained with phalloidin and DAPI and imaged. The confocal images were acquired using Zeiss AxioObserver Z1 microscope equipped with LSM700 laser scanning module (Zeiss, Thornwood, NY), at 40X magnification with 40x/1.3 Plan-Apochromat lens.

# RESULTS AND DISCUSSION

*Synthesis and characterization of pH-responsive block copolymers.* Ring opening polymerization of a pentafluorophenyl ester appended activated carbonate monomer (1), initiated by methoxy terminated poly (ethylene) glycol was employed to prepare the main chain of the PEG-PC block copolymer (Scheme 1).

**Scheme 1**. Synthetic route for the generation of pH responsive polymers

Block copolymers with pH-sensing side chains, i.e. **4** (PEG-AZB), **5** (PEG-Ile) and **6** (PEG-AZB-Ile) systems were synthesized from **3** by replacing the pentafluorophenol ester groups using the primary amines of 4-Amino-4'-dimethylaminoazobenzene (AZB) and Isoleucine (Ile, pKa 2.37) at post-polymerization step, respectively (**Scheme 1**). Synthesis and characterization of the precursor polymer (**3**) was carried out as reported earlier  $^{28, 41, 56}$ . These polymers were soluble in DMSO exclusively. Therefore, the  $^{1}$ H NMR was adopted to determine the number average molecular weight ( $M_n$ ), which is also a validated method to determine polymer molecular weights. Degree of polymerization ( $DP_n$ ) was obtained by dividing the  $M_n$  of the polymer by the molecular weight of the respective monomers. The number of side chain units were determined from  $^{1}$ H NMR spectra by comparing the ratio of the integrated area of the target peaks. The variation of  $M_n$  with composition of the polymers are presented in Table 1:

**Table 1**: Composition of pH-responsive block copolymers:

code	Hydrophilic	Hydrophobic	Side chain	m.w.	Number of side chain units
	block	block		(g/mol)	
4	PEG-5kDa	Poly(carbonate)	AZB	12.9	25
5	PEG-5kDa	Poly (carbonate)	Ile	13.4	18
6	PEG-5kDa	Poly (carbonate)	AZB + Ile	17.2	13 (AZB) + 9 (Ile)

Synthesis of the monomer (1) was carried out as reported by Hedricks et *al* <sup>57</sup>. All resulting polymers were characterized using <sup>1</sup>H NMR spectroscopy (**Fig. 1a for NMR** and Supporting information for synthetic description).

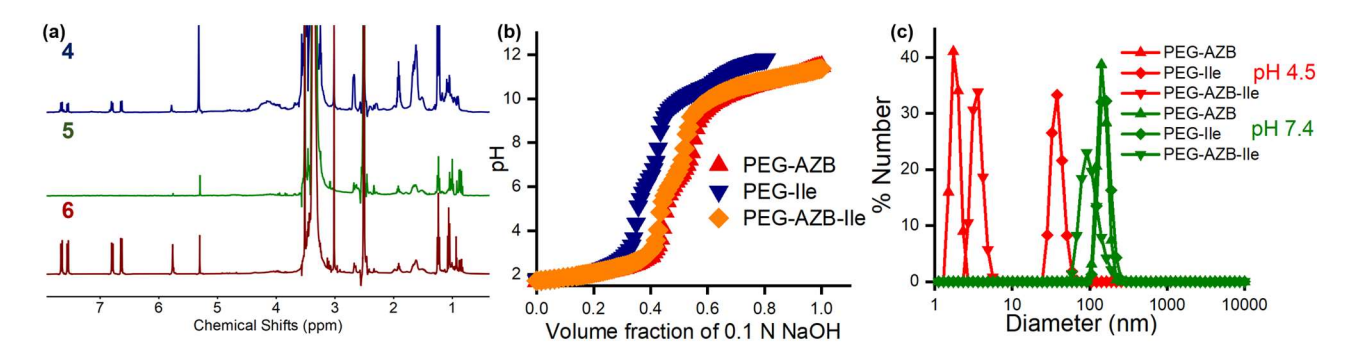


**Fig. 1:** (a) <sup>1</sup>H NMR spectra of block copolymers PEG-AZB (4), PEG-Ile (5) and PEG-AZB-Ile (6), (b) pH titration curves of the block copolymers (c) Size distribution of the nanoparticles at different pH. All nanoparticles showed pH-dependent reduction of particle size. Most significant (10-fold) reduction of size was observed with nanoparticles composed of polymer 4 and 6.

For polymer **4** and **6**, signals from the two aromatic protons from the ABZ moiety was observed between 7.1-7.7 ppm as doublets, while the protons of the methyl group from *-N (CH<sub>3</sub>)*<sup>2</sup> groups appeared at 2.84ppm as a broad singlet. <sup>19</sup>F NMR was used to identify if quantitative replacement of the pentafluorophenyl groups have taken place by the addition of amines. This reaction was followed by tracking the disappearance of signal in the region of -160 ppm (from pentafluorophenyl group of the precur-

sor molecule), which was no longer observed in the spectra of the products (Supporting information, Figure S2). During our reaction, we carefully controlled the inert atmosphere using Schlenk arrangement, and used anhydrous solvent. Therefore, we anticipate that PFP group will only be hydrolyzed by incoming nucleophilic attack by primary amines.

Self-assembly of pH-responsive block copolymers Block copolymers composed of hydrophobic domains connected to PEGs are well-established motif to form self-assembled structures in the form of micelles or polymersomes<sup>60</sup>. When the hydrophobic domain of a block copolymer is decorated with multiple copies of pH responsive side chains, such as tertiary amines, overall p $K_a$  value of the block copolymer regulates the reversible assembly-disassembly behavior of their assemblies as a function of pH. To determine the  $pK_a$  of the synthesized block copolymers, we titrated an acidic solution of each polymer against 0.1 N NaOH. In case of the PEG-AZB containing polymers (4 and 6) the color of the solution changed from dark orange in acidic media to yellow as the pH was gradually increased. From the titration curve of individual polymers (Fig. 1b, red and blue triangle) the  $pK_a$  value (pH at half inflection point) of 4 (hydrophobic block with AZB side chain) was found to be 6.49, whereas Ile containing block copolymer 5 showed an overall p $K_a$  value of 6.08. Co-conjugation of AZB and Ile at 1:1 feed ratio, as in **6**, showed a p $K_a$  value of 6.5 (Fig. 1b, orange diamond). These values led us to hypothesize that at the physiological pH of 7.4, less than 50% of ionizable side chains from all three copolymers will be protonated, and thereby will confer to systemic stability. Both AZB containing polymers (4 and 6) showed increased buffering capacity than the block copolymer conjugated exclusively with Ile. In aqueous solution, free Ile shows  $pK_a$  value of 2.32 (originating from the carboxylic acid) 9.76 (contributed from the amine groups) in its monomeric form. Our p $K_a$  measurement indicated that, conjugation of Ile through the N-termini to the polymer resulted in reduction of the p $K_a$  value of the polycarboxylate product compared to the monomer (from 9.76 to 6.08), due to conjugation of the amino acid to the PEGpolycarbonate backbone through the amide linkage via its primary amine.

Indeed, all synthesized block copolymers (4-6) were found to form self-assembled structures when using the nanoprecipitation method from a non-selective solvent like DMSO to a selective media, i.e. PBS maintained at pH 7.4. Dynamic Light Scattering (DLS) measurements at physiological pH showed the presence of particles with a number average hydrodynamic diameter within the range of 100 - 150 nm (Fig. 1c). More specifically, the particle size for polymers 4,5 and 6 were found to be 137.4 ( $\pm 8.1$ ) nm, 131.6 ( $\pm$ 11.9) nm and 114.3 ( $\pm$ 12.2) nm, respectively. Interestingly, when these particles were subjected to an acidic pH of 4.5, a significant (>10-fold) reduction of particle size was observed with nanoparticles composed of AZB containing copolymers (4 and 6). At pH 4.5, nanoparticles composed of these block copolymers displayed particles with an average hydrodynamic diameter of less than 20 nm for copolymer 4 and 6 The polydispersity PDI values in all cases were < 0.3. For nanoparticles composed of polymer 5, (i.e. Ile conjugated systems), average particle size was found to be 35.5 (±4.53) nm) (Fig. 1c). Particles prepared with Ile conjugated block copolymer did not show comparable reduction of hydrodynamic diameter compared to those prepared with 4 and 6, most likely due to protonation of carboxylate groups at lowered pH, leading to de-swelling and hydrophobic stabilization of the particles. Nanoparticles synthesized from different block copolymers did not show significant difference in their surface charge in terms of  $\zeta$ -potential. The surface charge density or of  $\zeta$ -potential of 4 was found to be -20.1 ( $\pm$ 1.5) mV, while 5 and 6 showed an average  $\zeta$ -potential of was -19.4 ( $\pm$  0.95) and -20.4 ( $\pm$ 1.2) mV, respectively. The reasons for the anionic zeta potential values can be explained in terms of the pendant group functionality (for Ile conjugated polymers) and net electron density (for AZB conjugated polymers)

Transmission electron microscopy (TEM) analysis revealed the formation of spherical, homogenous, and monodispersed nanoparticulate structures resulting from the assembly of copolymers **4-6**. The average size of the nanoparticles from TEM was observed to be  $\sim$  **4**, and  $\sim$  70 nm  $\pm$  12.9 nm and  $\sim$  60 nm  $\pm$  11.8 nm for copolymer **5** and **6**, respectively (**Fig. 2a-c**). When subjected to acidic pH (pH=4.5, these particles were found to collapse and a population of small structures (**Fig. 2a-c** bottom panel). Although

not prevalent with epithelial cells, pH inside macrophage lysosome is 4.7-4.8, although it can drop transiently as low as 4.5<sup>61</sup>. Therefore, we chose pH 4.5 as a representative acidic condition. The difference in hydrodynamic diameters in both pH values obtained by DLS and TEM-based measurements can be attributed to the shrinkage in the hydrophilic corona.

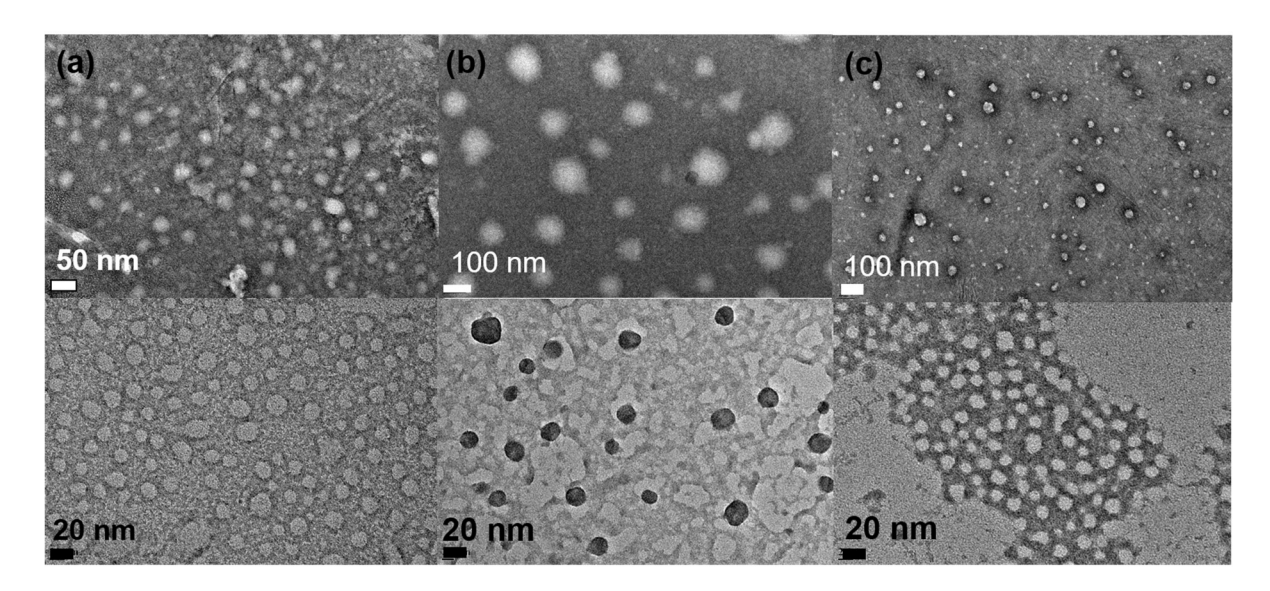


**Fig. 2.** (**Top panel**) TEM images at pH 7.4 of nanoparticles derived from (a) copolymer 4 with AZB, (b) copolymer 5 with conjugated Ile (c) and copolymer 6, co-conjugated to AZB and Ile. Corresponding images for each sample, incubated at acidic pH, are presented in the lower panel.

Plasma stability studies. We studied preliminary interactions of polymer nanoparticles with various plasma proteins to identify possible downstream effects of such interactions, which in turn form the basis of nanoparticle toxicity<sup>62</sup>. Calderon et al<sup>63</sup> and Chan and coworkers<sup>64</sup>, have reported that it is essential to comprehend such interactions which govern the therapeutic efficacy of nanoparticle-mediated drug delivery. A broad spectrum of protein components present in serum is encountered when nanoparticles are introduced in the blood stream leading to the formation of protein corona deposited on the surface of the latter. This nanoparticle–protein corona is a dynamic interface, that not only governs the interactions of nanomaterials with the physiological environment, but also directs stability, lifetime and down-stream pharmacological effects of nanoparticles <sup>65</sup>. To predict the fate of our engineered systems in the presence

of proteins encountered in the blood stream, we incubated each of these nanoparticle suspensions in 10% FBS and measured the particle size using DLS at regular intervals for 48 h. We observed that larger population of these particles remained stable although there was a slight increase in the hydrodynamic diameters post 24 hours which can be attributed to the protein corona and nanocarrier interactions (**Fig.** 3) <sup>66</sup> A small fraction of particulate aggregates were also observed, with an approximate diameter of 10 nm, origin of which cannot be pinpointed at this stage. Most likely these smaller particles could be resulting from aggregates of plasma proteins.

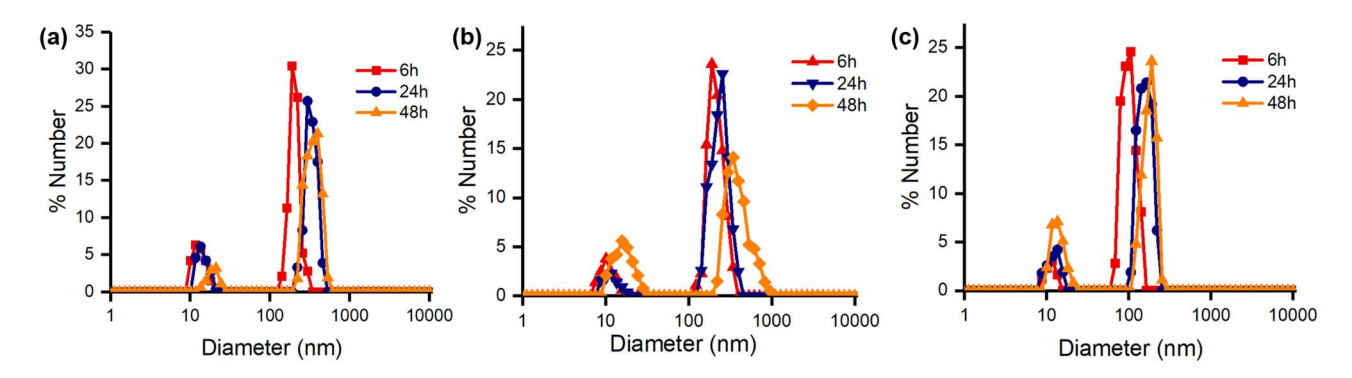


**Fig.3.** Plasma stability studies monitored by particle size distribution using DLS of nanoparticles generated from **(a)** AZB-containing block copolymer **(4)**, **(b)** Ile-rich block copolymer **(5)** and **(c)** copolymer co-functionalized with AZB and Ile **(6)**.

Determination of critical aggregation concentration (CAC) of block copolymer assemblies. After establishing the formation of self-assembled structures by block copolymers 4-6, we set out to investigate their critical aggregation concentration (CAC). Pyrene is a hydrophobic molecule used widely to determine the CAC of various polymeric constructs. It has been reported that the first ( $\lambda_{373}$  nm) and third ( $\lambda_{384}$  nm) peaks in the fluorescence emission spectra of pyrene are sensitive to the polarity of the environment and, the ratio of these two signals can therefore be used to determine the stability of association of block copolymers. We measured the fluorescence emission spectra at 373 and 384 nm and plotted the intensity ratio at these two wavelengths against polymer concentration. We observed a clear breakpoint for the concentration-dependent intensity changes for pyrene for all block copolymers at pH 7.4, but not at pH 4.5. (**Fig.4**).

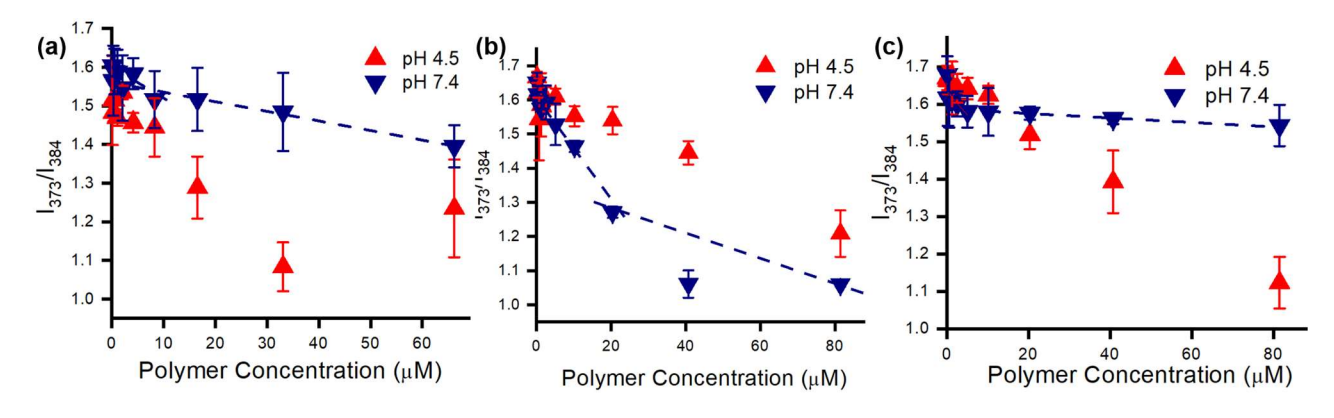


**Fig.4.** Plots of the ratio of I<sub>1</sub>/I<sub>3</sub> of pyrene as a function of polymer concentration of (a) PEG-AZB (4) (b) PEG-Ile (5) (c) PEG-AZB-Ile (6) at two different pH conditions (i.e., pH 7.4 and 4.5).

The point of intersection of the curves provided us with the CAC value for each polymer. While PEG-AZB (4) showed a CAC value of 3.56 x 10<sup>-6</sup> M and PEG-Ile (5) represented a CAC value of 20.7 x 10<sup>-6</sup> M, copolymer 6 exhibited a CAC value corresponding to 3.71 x 10<sup>-6</sup> M. We observed that, when the pH was lowered, the ratio of the first and third intensities decreased gradually over the range of concentrations used for pH 4.5, thereby indicating that at this pH, the polymer did not form any self-assembled structures. (Fig. 4b). The reason for relatively high CAC value for PEG-Ile system (5) can be attributed to preferential intramolecular hydrophobic interactions between Ile side chains within the same copolymer, preventing or weakening their intermolecular assembly.

Drug loading and Spatio-temporal release of encapsulated gemcitabine within block copolymer assemblies. To evaluate if these block copolymeric nanoparticles can be used as potential drug carriers, we evaluated their encapsulation and release properties towards a model drug, gemcitabine (GEM). As a nucleoside analog, GEM is used as one of the frontline chemotherapeutic agents against pancreatic cancer. We first evaluated the loading content of GEM in nanoparticles composed of block copolymer 4-6 (Table 2) using UV-Visible spectroscopy. We observed that loading content for nanoparticles composed of block copolymers bearing AZB were higher than those composed of block copolymers bearing Ile side chains, and comparable to pH-sensitive drug nanocarriers, which are composed of block copolymers bearing tertiary amines as pH-responding units.  $^{67-69}$  Multiple secondary interactions, such as  $\pi$ - $\pi$ ,

Van der Walls, and hydrophobic binding sites, provided by the constituent block copolymers could be attributed for such high capacity drug loading exhibited by these nanoparticles.

We also studied pH-dependent release of the encapsulated content from the nanoparticles as a function of time (**Fig. 5**). To design this experiment, we carried out vitro release studies of GEM from drug-loaded nanocarriers in the presence of 10% FBS dialyzed against buffer solution maintained at desired pH. To mimic the pH gradient of PDAC microenvironment we chose pH 7.4 and 4.5 (endosomallysosomal pH) to conduct the release experiment. We observed that in case of nanoparticles composed

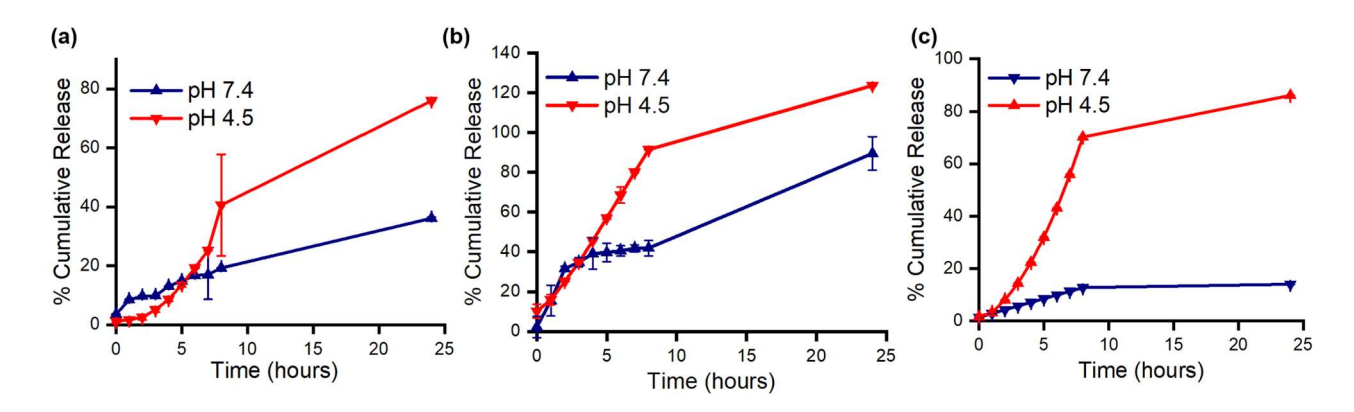


**Fig. 5.** Cumulative release of gemcitabine from nanoparticles derived from **(a)** PEG-AZB **(b)** PEG-Ile and **(c)** PEG-AZB-Ile systems, Error bars represent standard deviation of the average of three measurements.

of block copolymer 4 (i.e. PEG-AZB), ~ 30% of loaded GEM was released at physiological pH, where-as  $75.95 \pm 0.14\%$  of the drug was released at pH 4.5. We observed a biphasic release profile for most of the polymers, where the release rate was slowed between 8-24 h. For nano-constructs composed of block copolymers co-conjugated with AZB and Ile (polymer 6), <  $13.95 \pm 0.17\%$  GEM was released at pH 7.4 after 24 h, while  $86.1 \pm 0.01\%$  of GEM was released at the physiological pH over the same time frame. Nanoparticles composed of PEG-Ile systems did not exhibit an acute pH-sensitive drug release, accounting for only 20% difference in release between the pH levels of 7.4 and 4.5 over 24h (**Fig. 5a-c**). **Table 1** shows the  $t_{50\%}$  (time required to release 50% of the encapsulated content) from various formulations. Both CAC and drug release data indicates that polymer 4 bearing AZB side chains shows noticea-

ble pH-dependent assembly, loading content, and pH-programmable drug release properties. This pH-depended assembly-disassembly of nanoparticles composed of polymer 4 most likely stems from dimethylamino group of the azobenzene derivative (please see **Scheme 1**). As expected, nanoparticles composed of polymer 5 containing Ile side chains did not show any pH-responsive drug release properties. However, copolymer 6, which has both AZB and Ile side chains at 13 to 9 ratio) showed the highest resistance to drug release at neutral pH. This further strengthens our hypothesis that coupling the hydrophobic properties of amino acids with pH-sensing attributes of AZB-type systems enable to achieve tight packing of copolymeric nanoparticles, and controlled release of the encapsulated contents from these assemblies.

**Table 2**: Drug loading and t50% values for nanoparticles composed of copolymer 4-6:

Side chains at hydrophobic block <sup>a</sup>	Loading content (%)*	Loading efficiency (%) <sup>b</sup>	t <sub>50%</sub> (h)
AZB	$28.8 \pm 6.15$	$57.4 \pm 7.3$	12.19
Ile	$13.8 \pm 3.2$	$39.8 \pm 5.2$	4.42
AZB: Ile (13: 9)	$21.1 \pm 4.9$	$38.4 \pm 6.4$	6.63
dibutylamine <sup>67</sup>	$29 \pm 7.5$	$86 \pm 3.18$	6.98

<sup>&</sup>lt;sup>a</sup> PEG-PC block copolymer, PC is the hydrophobic block; AZB = 4-Amino-4'-dimethylaminoazobenzene, Ile = L-isoleucine. <sup>b</sup> Loading efficiency was calculated according to Equation 3 in supporting information. \* Calculated form UV-Vis spectroscopic analysis.

In vitro cytotoxicity and biocompatibility studies and cellular internalization studies. To investigate the cytotoxic effect of nanoparticle-bound GEM, we treated MIA PaCa-2 cells, a cell line reported to show KRAS mutation which is prevalent in PDAC, with GEM-loaded nanoparticles composed of copolymer 4-6. Cell viability assays using MTS were performed varying the concentration of encapsulated and free gemcitabine from 1 nM to 1 μM. Fig. 6a-c shows the effect of GEM-loaded and free nanoparticle toxicity against pancreatic cancer cell line, MIA PaCa-2, and a non-cancerous cell line from pancreas, HPNE that has been used as control. We observed that of all GEM-loaded nanoparticles composed of

block copolymers with AZB side chains, showed extensive cell death. For example, PEG-AZB-Ile nanoparticles released GEM that accounted for 30% cell viability at drug concentration of 1 µM post 72h incubation (**Figure 6a**), whereas GEM-loaded PEG-Ile nanoparticles showed almost equivalent extent of cytotoxicity compared to free GEM at similar concentration.

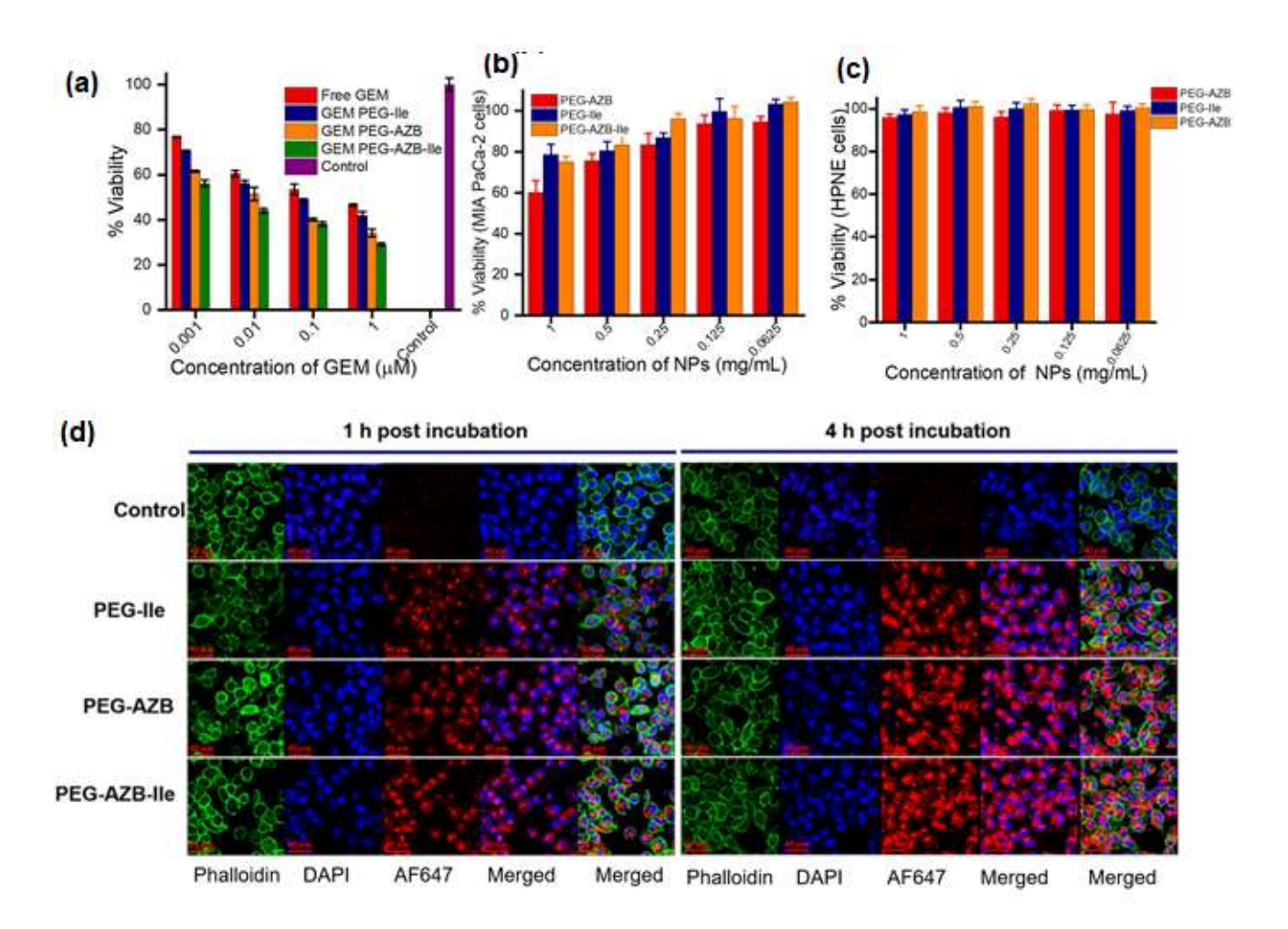


**Fig. 6 (a)** Cellular viability studies of MIA PaCa-2 treated with increasing GEM concentrations as nanocarrier formulation, or as free drug. Biocompatibility studies of bare polymeric nanocarriers on **(b)** MIA PaCa-2 cells and **(c)** HPNE cell line (N=3 for all assays). **(d)** Confocal microscopy images showing uptake of AF-647-labelled nanocarriers derived from different block copolymers 1 h post incubation (left panel) and 4 h post incubation (right panel) in MIA PaCa-2 cell lines.

To ascertain whether the cell death might have been induced by inherent toxicity of the nanoparticle-forming polymers, we also tested cytotoxicity of bare nanoparticles (no encapsulated GEM) composed of copolymer 4-6 on MIA PaCa-2 cell line (Fig. 6b). Various concentrations of each nanocarriers (ranging from 0.06 to 1 mg/mL) were used to treat the cells. All three nanoparticles, except the one composed of PEG-AZB, did not show significant toxic effect up to 1mg/mL against MIA PaCa-2 cells post 72 h incubation (Fig. 6b). Biocompatibility of the polymeric materials were tested on a non-cancerous, cell line, such as HPNE as control experiment. All drug-free nanoparticle formulations were found to be non-toxic within the tested range against non-cancerous cells, indicating excellent biocompatibility of the constituent polymers (Fig. 6c).

Fluorescent dye (Alexa 647) loaded nanocarriers were used to study the uptake and internalization in MIA PaCa-2 cells. A time dependent study was conducted to understand the internalization mechanism of nanocarriers composed of block copolymers **4-6**. We used a 2D culture of MIA PaCa-2 cells growing in log phase and incubated them with dye-labelled nanocarriers at different time points (1, 4 and 24 h). Post incubation, the cells were fixed and imaged using confocal microscopy. The images revealed that there was a time-dependent uptake of the nanoparticles and the fluorescence intensity of the dye increased from 1 h to 4 h (left and right panel of **Fig. 6d**). However, 24 h time point revealed a significant reduction of fluorescent intensity, most likely due to efflux of nanoparticles from cytoplasm (Supporting information, Figure S4).

# **CONCLUSION**

In this manuscript we report the design of a new type of pH-modulator, AZB, which when attached to the hydrophobic segment of an amphiphilic block copolymer, can promote assembly of the latter in a pH-dependent pattern. To further stabilize the system, we also explored the efficiency of a hydrophobic amino acid, Ile, which when connected to the same domain of the polymer, can tamper pH-dependent disassembly of the construct. We demonstrated the capacity of these newly designed block copolymers

to form self-assembled nanostructures at physiological pH that collapses under acidic pH conditions.

Thus, we anticipated that, these block copolymers will be suitable for preparation of pH-sensitive drug

delivery nanoparticles for pathological conditions, where the target site show extracellular matrix acidi-

fication, such as that happening in many solid tumors. To establish the feasibility, we studied nanoparti-

cle stability in blood plasma, their encapsulation and pH-sensitive release property of an anticancer

drug, and toxicity against cancer and healthy cells. We observed GEM-loaded nanoparticles composed

of AZB-appended block copolymers were effective in lowering cancer cell proliferation and showed

time-dependent intracellular uptake. Drug free nanoparticles were found to be non-toxic to non-

cancerous cell lines. We envision that azo-dye derivative conjugated PEG-b-poly (carbonate) block co-

polymers can bring forward new design principles for synthesizing pH-responsive nanoplatform with

high content drug encapsulation, and controlled drug release properties.

ASSOCIATED CONTENT

Supporting information is available free of charge via the Internet at http://pubs.acs.org.

**AUTHOR INFORMATION** 

**Corresponding Author** 

Department of Coatings and Polymeric Materials, 1735 Research Park Drive, Fargo, North Dakota,

USA. Fax: 701-231-6283; Tel: 701-231-6283; E-mail: mohiuddin.quadir@ndsu.edu

**Author Contributions** 

The manuscript was written through contributions of all authors. / All authors have given approval to the

final version of the manuscript.

**Funding Sources** 

This research was supported by NIH grant number 1P20 GM109024 from the National Institute of Gen-

eral Medical Sciences (NIGMS). TEM material is based upon work supported by the NSF under Grant

No. 0923354. Funding for the Core Biology Facility used in this publication was made possible by NIH Grant Number 2P20 RR015566 from the National Center for Research Resources.

Any opinions, findings, and conclusions or recommendations expressed are those of the author(s) and do not necessarily reflect the views of the NIH.

# ACKNOWLEDGMENT

We would like to acknowledge Mr. Tom Gustad for his help with plasma separation and related analyses. Dr. Pawel Borowicz is acknowledged for his support with confocal microscopy image processing. The authors would like to thank Dr. Scott Payne and Jayma Moore for TEM imaging.

# **ABBREVIATIONS**

GEM, gemcitabine; NP, nanoparticle; CAC, Critical Aggregation Constant; DLS, Dynamic Light Scattering; TEM, Transmission Electron Microscopy; Ile, Isoleucine; PEG, poly(ethylene)glycol; AZB, 4-Amino-4'-dimethylaminoazobenzene

- 1. Khemtong, C.; Kessinger, C. W.; Gao, J., Polymeric nanomedicine for cancer MR imaging and drug delivery. *Chemical Communications* **2009**, (24), 3497-3510.
- 2. Oberoi, H. S.; Nukolova, N. V.; Kabanov, A. V.; Bronich, T. K., Nanocarriers for delivery of platinum anticancer drugs. *Advanced Drug Delivery Reviews* **2013**, *65* (13), 1667-1685.
- 3. Brigger, I.; Dubernet, C.; Couvreur, P., Nanoparticles in cancer therapy and diagnosis. *Advanced Drug Delivery Reviews* **2002**, *54* (5), 631-651.
- 4. Mitragotri, S., In Drug Delivery, Shape Does Matter. *Pharmaceutical Research* **2009**, *26* (1), 232-234.
- 5. Li, F.; Danquah, M.; Mahato, R. I., Synthesis and Characterization of Amphiphilic Lipopolymers for Micellar Drug Delivery. *Biomacromolecules* **2010**, *11* (10), 2610-2620.
- 6. Jain, R. K., Transport of molecules in the tumor interstitium: a review. *Cancer Res* **1987**, *47* (12), 3039-51.
- 7. Champion, J. A.; Katare, Y. K.; Mitragotri, S., Particle shape: A new design parameter for micro- and nanoscale drug delivery carriers. *Journal of Controlled Release* **2007**, *121* (1), 3-9.
- 8. Jain, R. K., Transport of molecules across tumor vasculature. *Cancer Metastasis Rev* **1987**, *6* (4), 559-93.
- 9. Maeda, H.; Wu, J.; Sawa, T.; Matsumura, Y.; Hori, K., Tumor vascular permeability and the EPR effect in macromolecular therapeutics: a review. *J Control Release* **2000**, *65* (1-2), 271-84.
- 10. Maeda, H., Polymer therapeutics and the EPR effect. J Drug Target 2017, 25 (9-10), 781-785.
- 11. Prabhakar, U.; Maeda, H.; Jain, R. K.; Sevick-Muraca, E. M.; Zamboni, W.; Farokhzad, O.
- C.; Barry, S. T.; Gabizon, A.; Grodzinski, P.; Blakey, D. C., Challenges and key considerations of the enhanced permeability and retention effect for nanomedicine drug delivery in oncology. In *Cancer Res*, (c)2013 AACR.: United States, 2013; Vol. 73, pp 2412-7.
- 12. Fleige, E.; Quadir, M. A.; Haag, R., Stimuli-responsive polymeric nanocarriers for the controlled transport of active compounds: Concepts and applications. *Advanced Drug Delivery Reviews* **2012**, *64* (9), 866-884.
- 13. Haag, R.; Kratz, F., Polymer Therapeutics: Concepts and Applications. *Angewandte Chemie International Edition* **2006**, *45* (8), 1198-1215.
- 14. Mura, S.; Nicolas, J.; Couvreur, P., Stimuli-responsive nanocarriers for drug delivery. *Nature Materials* **2013**, *12* (11), 991-1003.
- 15. Chauhan, V. P.; Jain, R. K., Strategies for advancing cancer nanomedicine. *Nat Mater* **2013**, *12* (11), 958-962.
- 16. Fukumura, D.; Jain, R. K., Tumor microvasculature and microenvironment: Targets for antiangiogenesis and normalization. *Microvascular Research* **2007**, *74* (2), 72-84.
- 17. Quadir, M. A.; Morton, S. W.; Deng, Z. J.; Shopsowitz, K. E.; Murphy, R. P.; Epps, T. H.; Hammond, P. T., PEG–Polypeptide Block Copolymers as pH-Responsive Endosome-Solubilizing Drug Nanocarriers. *Molecular Pharmaceutics* **2014**, *11* (7), 2420-2430.
- 18. Ray, P.; Nair, G.; Ghosh, A.; Banerjee, S.; Golovko, M. Y.; Banerjee, S. K.; Reindl, K. M.; Mallik, S.; Quadir, M., Microenvironment-sensing, nanocarrier-mediated delivery of combination chemotherapy for pancreatic cancer. *Journal of Cell Communication and Signaling* **2019**.
- 19. Akakura, N.; Kobayashi, M.; Horiuchi, I.; Suzuki, A.; Wang, J.; Chen, J.; Niizeki, H.; Kawamura, K.-i.; Hosokawa, M.; Asaka, M., Constitutive Expression of Hypoxia-inducible Factor-1α Renders Pancreatic Cancer Cells Resistant to Apoptosis Induced by Hypoxia and Nutrient Deprivation. *Cancer Research* **2001**, *61* (17), 6548-6554.
- 20. Chen, Q.; Feng, L.; Liu, J.; Zhu, W.; Dong, Z.; Wu, Y.; Liu, Z., Intelligent Albumin–MnO2 Nanoparticles as pH-/H2O2-Responsive Dissociable Nanocarriers to Modulate Tumor Hypoxia for Effective Combination Therapy. *Advanced Materials* **2016**, *28* (33), 7129-7136.
- 21. Vaupel, P.; Mayer, A., Hypoxia in cancer: significance and impact on clinical outcome. *Cancer and Metastasis Reviews* **2007**, *26* (2), 225-239.

- 22. Johnstone, R. W., Histone-deacetylase inhibitors: novel drugs for the treatment of cancer. *Nat Rev Drug Discov* **2002**, *1* (4), 287-99.
- 23. Weidle, U. H.; Grossmann, A., Inhibition of histone deacetylases: a new strategy to target epigenetic modifications for anticancer treatment. *Anticancer Res* **2000**, *20* (3a), 1471-85.
- 24. Calderón, M.; Quadir, M. A.; Strumia, M.; Haag, R., Functional dendritic polymer architectures as stimuli-responsive nanocarriers. *Biochimie* **2010**, *92* (9), 1242-1251.
- 25. Krämer, M.; Stumbé, J.-F.; Türk, H.; Krause, S.; Komp, A.; Delineau, L.; Prokhorova, S.; Kautz, H.; Haag, R., pH-Responsive Molecular Nanocarriers Based on Dendritic Core-Shell Architectures. *Angewandte Chemie International Edition* **2002**, *41* (22), 4252-4256.
- 26. Xu, S.; Luo, Y.; Graeser, R.; Warnecke, A.; Kratz, F.; Hauff, P.; Licha, K.; Haag, R., Development of pH-responsive core—shell nanocarriers for delivery of therapeutic and diagnostic agents. *Bioorganic & Medicinal Chemistry Letters* **2009**, *19* (3), 1030-1034.
- 27. Nowag, S.; Haag, R., pH-Responsive Micro- and Nanocarrier Systems. *Angewandte Chemie International Edition* **2014**, *53* (1), 49-51.
- 28. Ray, P.; Confeld, M.; Borowicz, P.; Wang, T.; Mallik, S.; Quadir, M., PEG-b-poly (carbonate)-derived nanocarrier platform with pH-responsive properties for pancreatic cancer combination therapy. *Colloids and Surfaces B: Biointerfaces* **2019**, *174*, 126-135.
- 29. Ray, P.; Ferraro, M.; Haag, R.; Quadir, M., Dendritic Polyglycerol-Derived Nano-Architectures as Delivery Platforms of Gemcitabine for Pancreatic Cancer. *Macromol Biosci* **2019**, *19* (7), e1900073.
- 30. Kimbrough, C. W.; Khanal, A.; Zeiderman, M.; Khanal, B. R.; Burton, N. C.; McMasters, K. M.; Vickers, S. M.; Grizzle, W. E.; McNally, L. R., Targeting Acidity in Pancreatic Adenocarcinoma: Multispectral Optoacoustic Tomography Detects pH-Low Insertion Peptide Probes <em>In Vivo</em>. Clinical Cancer Research 2015, 21 (20), 4576.
- 31. Martin, G. R.; Jain, R. K., Noninvasive Measurement of Interstitial pH Profiles in Normal and Neoplastic Tissue Using Fluorescence Ratio Imaging Microscopy. *Cancer Research* **1994**, *54* (21), 5670.
- 32. Bailey, J. M.; Mohr, A. M.; Hollingsworth, M. A., Sonic hedgehog paracrine signaling regulates metastasis and lymphangiogenesis in pancreatic cancer. *Oncogene* **2009**, *28* (40), 3513-3525.
- 33. Gerweck, L. E.; Seetharaman, K., Cellular pH Gradient in Tumor <em>versus</em> Normal Tissue: Potential Exploitation for the Treatment of Cancer. *Cancer Research* **1996**, *56* (6), 1194.
- 34. Zhou, K.; Wang, Y.; Huang, X.; Luby-Phelps, K.; Sumer, B. D.; Gao, J., Tunable, ultrasensitive pH-responsive nanoparticles targeting specific endocytic organelles in living cells. *Angewandte Chemie (International ed. in English)* **2011**, *50* (27), 6109-6114.
- 35. Matsumoto, A.; Yoshida, R.; Kataoka, K., Glucose-Responsive Polymer Gel Bearing Phenylborate Derivative as a Glucose-Sensing Moiety Operating at the Physiological pH. *Biomacromolecules* **2004**, *5* (3), 1038-1045.
- 36. Takemoto, H.; Miyata, K.; Hattori, S.; Ishii, T.; Suma, T.; Uchida, S.; Nishiyama, N.; Kataoka, K., Acidic pH-responsive siRNA conjugate for reversible carrier stability and accelerated endosomal escape with reduced IFNalpha-associated immune response. *Angew Chem Int Ed Engl* **2013**, *52* (24), 6218-21.
- 37. Oishi, M.; Sasaki, S.; Nagasaki, Y.; Kataoka, K., pH-Responsive Oligodeoxynucleotide (ODN)–Poly(Ethylene Glycol) Conjugate through Acid-Labile β-Thiopropionate Linkage: Preparation and Polyion Complex Micelle Formation. *Biomacromolecules* **2003**, *4* (5), 1426-1432.
- 38. Lynn, D. M.; Amiji, M. M.; Langer, R., pH-Responsive Polymer Microspheres: Rapid Release of Encapsulated Material within the Range of Intracellular pH. *Angewandte Chemie International Edition* **2001**, *40* (9), 1707-1710.
- 39. Jain, R. K.; Stylianopoulos, T., Delivering nanomedicine to solid tumors. *Nature reviews*. *Clinical oncology* **2010**, *7* (11), 653-664.
- 40. Engler, A. C.; Bonner, D. K.; Buss, H. G.; Cheung, E. Y.; Hammond, P. T., The synthetic tuning of clickable pH responsive cationic polypeptides and block copolypeptides. *Soft Matter* **2011**, *7* (12), 5627-5637.

- 41. Engler, A. C.; Chan, J. M. W.; Coady, D. J.; O'Brien, J. M.; Sardon, H.; Nelson, A.; Sanders, D. P.; Yang, Y. Y.; Hedrick, J. L., Accessing New Materials through Polymerization and Modification of a Polycarbonate with a Pendant Activated Ester. *Macromolecules* **2013**, *46* (4), 1283-1290.
- 42. Greenwald, R. B.; Conover, C. D.; Choe, Y. H., Poly(ethylene glycol) conjugated drugs and prodrugs: a comprehensive review. *Crit Rev Ther Drug Carrier Syst* **2000**, *17* (2), 101-61.
- 43. Matsumoto, Y.; Nichols, J. W.; Toh, K.; Nomoto, T.; Cabral, H.; Miura, Y.; Christie, R. J.; Yamada, N.; Ogura, T.; Kano, M. R.; Matsumura, Y.; Nishiyama, N.; Yamasoba, T.; Bae, Y. H.; Kataoka, K., Vascular bursts enhance permeability of tumour blood vessels and improve nanoparticle delivery. *Nat Nanotechnol* **2016**, *11* (6), 533-538.
- 44. Zhou, K.; Liu, H.; Zhang, S.; Huang, X.; Wang, Y.; Huang, G.; Sumer, B. D.; Gao, J., Multicolored pH-Tunable and Activatable Fluorescence Nanoplatform Responsive to Physiologic pH Stimuli. *Journal of the American Chemical Society* **2012**, *134* (18), 7803-7811.
- 45. Weinberg, B. D.; Blanco, E.; Gao, J., Polymer Implants for Intratumoral Drug Delivery and Cancer Therapy. *Journal of Pharmaceutical Sciences* **2008**, *97* (5), 1681-1702.
- 46. Ma, X.; Wang, Y.; Zhao, T.; Li, Y.; Su, L.-C.; Wang, Z.; Huang, G.; Sumer, B. D.; Gao, J., Ultra-pH-Sensitive Nanoprobe Library with Broad pH Tunability and Fluorescence Emissions. *Journal of the American Chemical Society* **2014**, *136* (31), 11085-11092.
- 47. Kataoka, K.; Harada, A.; Nagasaki, Y., Block copolymer micelles for drug delivery: design, characterization and biological significance. *Adv Drug Deliv Rev* **2001**, *47* (1), 113-31.
- 48. Dirksen, A.; Zuidema, E.; Williams, R. M.; De Cola, L.; Kauffmann, C.; Vögtle, F.; Roque, A.; Pina, F., Photoactivity and pH Sensitivity of Methyl Orange Functionalized Poly(Propyleneamine) Dendrimers. *Macromolecules* **2002**, *35* (7), 2743-2747.
- 49. Albertazzi, L.; Storti, B.; Marchetti, L.; Beltram, F., Delivery and Subcellular Targeting of Dendrimer-Based Fluorescent pH Sensors in Living Cells. *Journal of the American Chemical Society* **2010**, *132* (51), 18158-18167.
- 50. Guo, J.; Yang, W.; Deng, Y.; Wang, C.; Fu, S., Organic-Dye-Coupled Magnetic Nanoparticles Encaged Inside Thermoresponsive PNIPAM Microcapsules. *Small* **2005**, *1* (7), 737-743.
- 51. Bilalis, P.; Tziveleka, L.-A.; Varlas, S.; Iatrou, H., pH-Sensitive nanogates based on poly (Lhistidine) for controlled drug release from mesoporous silica nanoparticles. *Polymer Chemistry* **2016**, *7* (7), 1475-1485.
- 52. Hwang, J.-H.; Choi, C. W.; Kim, H.-W.; Kim, D. H.; Kwak, T. W.; Lee, H. M.; Kim, C. H.; Chung, C. W.; Jeong, Y.-I.; Kang, D. H., Dextran-b-poly(L-histidine) copolymer nanoparticles for phresponsive drug delivery to tumor cells. *International journal of nanomedicine* **2013**, *8*, 3197-3207.
- 53. El-Sayed, A.; Futaki, S.; Harashima, H., Delivery of Macromolecules Using Arginine-Rich Cell-Penetrating Peptides: Ways to Overcome Endosomal Entrapment. *The AAPS Journal* **2009**, *11* (1), 13-22.
- 54. Bauri, K.; De, P.; Shah, P. N.; Li, R.; Faust, R., Polyisobutylene-Based Helical Block Copolymers with pH-Responsive Cationic Side-Chain Amino Acid Moieties by Tandem Living Polymerizations. *Macromolecules* **2013**, *46* (15), 5861-5870.
- 55. Zhu, B. Y.; Zhou, N. E.; Kay, C. M.; Hodges, R. S., Packing and hydrophobicity effects on protein folding and stability: effects of beta-branched amino acids, valine and isoleucine, on the formation and stability of two-stranded alpha-helical coiled coils/leucine zippers. *Protein Sci* **1993**, *2* (3), 383-94.
- 56. Liu, J.; Liu, W.; Weitzhandler, I.; Bhattacharyya, J.; Li, X.; Wang, J.; Qi, Y.; Bhattacharjee, S.; Chilkoti, A., Ring-Opening Polymerization of Prodrugs: A Versatile Approach to Prepare Well-Defined Drug-Loaded Nanoparticles. *Angewandte Chemie International Edition* **2015**, *54* (3), 1002-1006.
- 57. Sanders, D. P.; Fukushima, K.; Coady, D. J.; Nelson, A.; Fujiwara, M.; Yasumoto, M.; Hedrick, J. L., A Simple and Efficient Synthesis of Functionalized Cyclic Carbonate Monomers Using a Versatile Pentafluorophenyl Ester Intermediate. *Journal of the American Chemical Society* **2010**, *132* (42), 14724-14726.

- 58. Bilati, U.; Allémann, E.; Doelker, E., Development of a nanoprecipitation method intended for the entrapment of hydrophilic drugs into nanoparticles. *European Journal of Pharmaceutical Sciences* **2005**, *24* (1), 67-75.
- 59. Ray, P.; Alhalhooly, L.; Ghosh, A.; Choi, Y.; Banerjee, S.; Mallik, S.; Banerjee, S.; Quadir, M., Size-Transformable, Multifunctional Nanoparticles from Hyperbranched Polymers for Environment-Specific Therapeutic Delivery. *ACS Biomaterials Science & Engineering* **2019**, *5* (3), 1354-1365.
- 60. Gao, W.; Chan, J. M.; Farokhzad, O. C., pH-Responsive Nanoparticles for Drug Delivery. *Molecular Pharmaceutics* **2010**, *7* (6), 1913-1920.
- 61. Ohkuma, S.; Poole, B., Fluorescence probe measurement of the intralysosomal pH in living cells and the perturbation of pH by various agents. *Proc Natl Acad Sci U S A* **1978**, *75* (7), 3327-31.
- 62. Saptarshi, S. R.; Duschl, A.; Lopata, A. L., Interaction of nanoparticles with proteins: relation to bio-reactivity of the nanoparticle. *Journal of Nanobiotechnology* **2013**, *11* (1), 26.
- 63. Miceli, E.; Kar, M.; Calderón, M., Interactions of organic nanoparticles with proteins in physiological conditions. *Journal of Materials Chemistry B* **2017**, *5* (23), 4393-4405.
- 64. Walkey, C. D.; Chan, W. C. W., Understanding and controlling the interaction of nanomaterials with proteins in a physiological environment. *Chemical Society Reviews* **2012**, *41* (7), 2780-2799.
- 65. Giulimondi, F.; Digiacomo, L.; Pozzi, D.; Palchetti, S.; Vulpis, E.; Capriotti, A. L.; Chiozzi, R. Z.; Laganà, A.; Amenitsch, H.; Masuelli, L.; Mahmoudi, M.; Screpanti, I.; Zingoni, A.; Caracciolo, G., Interplay of protein corona and immune cells controls blood residency of liposomes. *Nature Communications* **2019**, *10* (1), 3686.
- 66. Casals, E.; Pfaller, T.; Duschl, A.; Oostingh, G. J.; Puntes, V., Time Evolution of the Nanoparticle Protein Corona. *ACS Nano* **2010**, *4* (7), 3623-3632.
- 67. Ray, P.; Confeld, M.; Borowicz, P.; Wang, T.; Mallik, S.; Quadir, M., PEG-b-poly (carbonate)-derived nanocarrier platform with pH-responsive properties for pancreatic cancer combination therapy. *Colloids Surf B Biointerfaces* **2018**, *174*, 126-135.
- 68. Arias, J. L.; Reddy, L. H.; Couvreur, P., Polymeric nanoparticulate system augmented the anticancer therapeutic efficacy of gemcitabine. *Journal of Drug Targeting* **2009**, *17* (8), 586-598.
- 69. Xu, H.; Paxton, J.; Lim, J.; Li, Y.; Zhang, W.; Duxfield, L.; Wu, Z., Development of High-Content Gemcitabine PEGylated Liposomes and Their Cytotoxicity on Drug-Resistant Pancreatic Tumour Cells. *Pharmaceutical Research* **2014**, *31* (10), 2583-2592.